Effect of Axial Torsion on sp Carbon Atomic Wires

Luca Ravagnan,[1,2] Nicola Manini,[1,3] Eugenio Cinquanta,[1,2,*] Giovanni Onida,[1,3,†] Davide Sangalli,[1,3] Carlo Motta,[1,3] Michele Devetta,[1,2] Andrea Bordoni,[1,2] Paolo Piseri,[1,2] and Paolo Milani[1,2,‡]

[1]*Dipartimento di Fisica, Università degli Studi di Milano, Via Celoria 16, 20133 Milano, Italy*

[2]*CIMAINA, Via Celoria 16, 20133 Milano, Italy*

[3]*European Theoretical Spectroscopy Facility, Via Celoria 16, 20133 Milano, Italy*

(Received 9 February 2009; published 17 June 2009)

Ab initio calculations within density-functional theory combined with experimental Raman spectra on cluster-beam deposited pure-carbon films provide a consistent picture of sp-carbon chains stabilized by sp^3 or sp^2 terminations, the latter being sensitive to torsional strain. This unexplored effect promises many exciting applications since it allows one to modify the conductive states near the Fermi level and to switch on and off the on-chain π-electron magnetism.

DOI: 10.1103/PhysRevLett.102.245502 PACS numbers: 61.48.De, 31.15.A−, 36.20.Ng, 81.07.−b

Postsilicon electronics has seen the recent opening of entirely new perspectives along the way of carbon-based devices. By proper nanoscale design, entirely carbon-made transistors have been realized [1]. Future applications have been devised, including bionanotechnology ones such as devices for fast DNA reading [2]. Even considering only well-demonstrated applications, the potential of carbon-based electronics is undoubtedly enormous, as testified by the realization of nonvolatile memories based on two-terminal atomic-scale switches [3] and bistable graphitic memories [4]. Specifically, these structural memory effects have been explained by the formation of carbon chains made by a few aligned sp-hybridized atoms bridging a nanometric gap [3].

In this context, the production of pure-carbon nanostructured films with coexisting sp and sp^2 hybridization [5,6] opens the exciting possibility to tailor complex carbon-based nanostructures with linear chains made of sp-hybridized C atoms connecting graphitic nano-objects. However, despite several theoretical studies devoted to sp-carbon nanowires [7–10] classified either as cumulenes (virtually conducting, characterized by double C-C bonds) or polyynes (large-gap insulators with alternating single and triple bonds), the implications associated with the nanoscale geometrical manipulation of hybrid $sp + sp^2$ carbon systems are still largely unexplored.

In this Letter we show that sp nanowires can be stabilized effectively by termination on graphitic nanofragments, and that in the resulting structures the $\simeq$1 nm-long linear atomic chains can be torsionally stiff, due to the broken axial symmetry with staggered π bonds. This stiffness is rich in consequences. We explore here how the structural, vibrational, and electronic properties of such chains are affected by the nature and *geometry* of the termination. In particular, we show that sp^2 bonding to graphitic fragments and graphene nanoribbons (NRs) produces remarkably stable structures, with cumulene-type chains displaying a non-negligible bond-length alternation (BLA), so that the traditional categories of polyynes (alternating single-triple bonds, yielding a large BLA) and cumulenes (double bonds, negligible BLA) appear too simplistic for the description of these systems. Torsional deformations are found to affect the BLA, electronic gap, stretching vibrational frequencies, and spin magnetization of the chains.

We study these effects in realistic nanostructures, including carbon chains bound to graphitic fragments. We perform all calculations within density-functional theory in the local spin density approximation, using a plane-wave basis as implemented in the ESPRESSO [11] suite [12].

Figure 1 displays a few of the studied systems involving either sp^2 or sp^3 bonding of a sp nanowire with an sp^2-type fragment. The chosen end-capping nanostructures include planar graphitic fragments and closed-cage clusters (here, C_{20}, the most curved fullerene). These

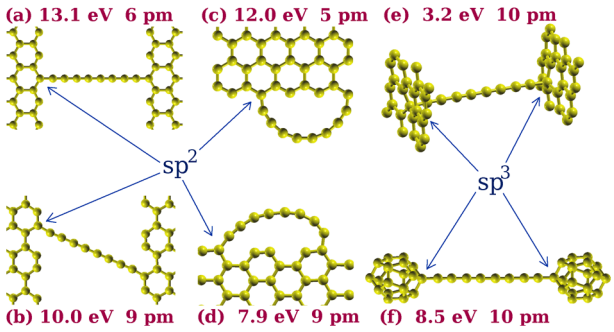

FIG. 1 (color online). A few representative structures involving an 8-atom sp-bonded carbon chain terminated on sp^2-carbon fragments [(a–e) NRs, (f) C_{20}]. Either edge termination [(a–d) sp^2-like] or termination on an internal atom of the fragment [(e–f) sp^3-like] is possible. Binding energies (with respect to the uncapped straight chain plus fully relaxed sp^2 fragments) and BLA (expressed in picometers) are reported.

structures are intended to represent typical interfaces present in the nanostructured films produced by cluster-beam deposition [14].

The nature of the terminal bonding turns out to be crucial in determining the structure and electronic properties of the wire. An sp^2-kind termination produces remarkably stable cumulene-type structures (between 7.9 and 13 eV for the formation of the two new bonds), characterized by a BLA between 5 and 9 pm [15]. The computed binding energy should be compared with the energy per bond of 2.1 eV that we obtain for a lateral attachment of the same chain to the ribbon edge, and with the formation energy of graphene edges [13,16]; moreover, it is much larger than the reported binding energies of carbon chains inside nanotubes [17]. Figure 1 also shows that the mere value of the BLA does not allow one to distinguish between carbon chains which would be traditionally classified as cumulenic (a–d) or polyynic (e–f) according to their terminations.

For the sake of comparison we also consider standard cumulenes and polyynes, in the form of isolated carbon chains stabilized by hydrogen terminations. Polyynes C_nH_2 have been synthesized up to a considerable length ($n = 20$) [18,19] in liquid and solid matrices, and also with different stabilizing end groups. Their electronic and vibrational properties as isolated species have been characterized extensively, mainly by electronic and Raman spectroscopy [19,20]. On the other hand, cumulenes $C_{n+2}H_4$ can be seen as C_n sp chains terminated by CH_2 groups, yielding all double C = C bonds. Cumulenes are more elusive and less well characterized than polyynes, due to their fragility. Recently, short cumulenic chains have been synthesized in their basic forms, butatriene and hexapentaene [21]. Cumulenic chains are often produced in conjunction with more complex terminations than simple CH_2 units, including CPh_2, i.e., 1,1 diphenyl ethyl (DPE) groups [22], which we also simulate.

As one could infer from elementary valence bond or tight-binding considerations, depending on the number n of carbons being even/odd, sp^2-terminated cumulenes assume a D_{2h} (planar) or a D_{2d} (staggered) ground-state geometry, respectively, due to the alternating orientation of the π bonds along the chain [21]. Similarly, chains bonded to sp^2 structures are affected by the relative orientation of their terminations. Indeed, a memory of the orientation of the bonds of the terminating sp^2 carbon propagates along the sp-hybridized chain, so that even-n chains tend to relax to a configuration where the termination sp^2 planes coincide, while odd-n chains tend to keep their terminations at a twist angle $\theta = 90°$. As a consequence, despite their purely one-dimensional nature, sp^2-terminated carbon chains display a nonvanishing torsional stiffness, no matter if they are straight or bent as in Figs. 1(c) and 1(d). In contrast, ideally polyynic chains (i.e., those terminated at a sp^3 site, with a pure single-triple bond alternation) are almost completely free to rotate around their axis, but suffer from an obvious frustration when the number of atoms is odd since the long-short bond alternation must swap at their middle [23]. Importantly, in nanostructured cluster-assembled carbon characterized by a complex three-dimensional arrangement of graphitic fragments and sp chains [5,6], a large number of the chains binding to sp^2 structures are not free to relax their terminations to the preferred angular geometry, and must hence be expected to be, in general, strained torsionally.

Since the simulation of carbon-only structures such as graphene NR bridged by chains allows us to investigate a few relative angular arrangements only, we extend our study also to chains with simpler saturating ligands, namely, CH_2 and DPE. The latter turns out to reproduce better the behavior of a large (potentially semi-infinite) graphitic fragment, which, at variance with CH_2, shares with the chain only a fraction of its unsaturated p_z electron, which is partly delocalized over an extended aromatic sp^2 structure.

Figure 2 summarizes the influence of different end groups on the BLA and, for sp^2 termination, the torsional strain energy and the Kohn-Sham electronic gap of even-n chains as a function of θ. Interestingly, largely strained chains undergo a magnetic instability, turning spin polarized. The reason is the quasidegeneracy of two π-bonding or -antibonding electronic levels near the Fermi energy illustrated by the closing of the gap [Fig. 2(b)]. Remarkably, in even-numbered chains of all considered lengths, no matter if CH_2 or DPE terminated, the switching to a spin-polarized configuration takes place at the same twist angle $\theta_s \simeq 79°$, highlighted in Fig. 2 [24]. This θ_s

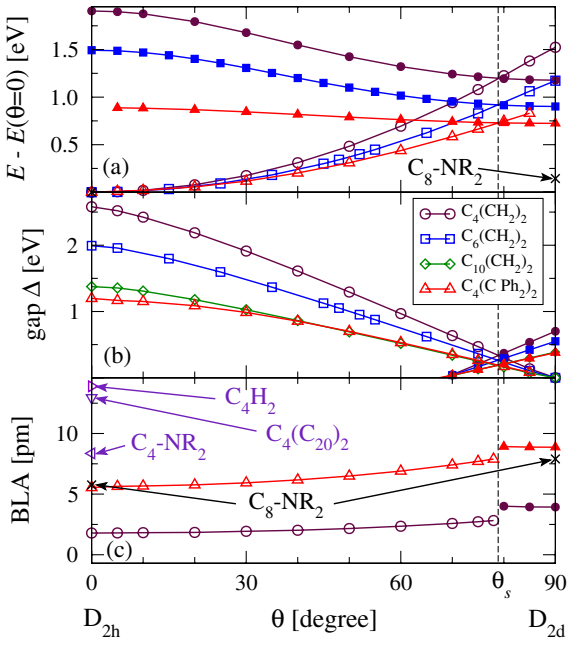

FIG. 2 (color online). Total torsional energy (a), Kohn-Sham electronic gap (b), and bond-length alternation (c) as a function of the twist angle θ for representative even-numbered sp-carbon chains with different terminations. Open (filled) symbols refer to the low- (high-)spin electronic configurations.

invariance implies that the energy gap Δ and the exchange splitting of the electrons near the Fermi level scale in the same way.

Calculations show that the BLA of the sp^2-terminated chains varies substantially with the nature of the termination itself [10]. The length of the extremal bond (i.e., the one connecting the last sp carbon with sp^2/sp^3-hybridized ligand), which correlates with the BLA, is minimal in the case of a simple CH_2 termination, but increases substantially in DPE-terminated chains, assumes even larger values in NR-terminated wires, and is maximum for polyynic-type terminations [see Figs. 1 and 2(c)]. The torsional barrier is consistently smaller for NR terminations, as indicated by the cross at $\theta = 90°$ in Fig. 2(a).

In the light of the above results, chain-termination details are expected to influence the vibrational properties as well. The latter offer an invaluable opportunity to check if the considered structures are representative of those present in nanostructured cluster-assembled films, for which Raman spectra are the main experimental evidence of the presence of linear carbon chains. Indeed, in previous works some of us showed that the Raman fingerprint of carbyne chains in sp-sp^2 carbon is characterized by a broad feature, with 2 components C1 and C2 peaked at 1980 and 2100 cm^{-1}, respectively [5,6]. Traditionally these features were attributed generically to cumulenes (C1) and polyynes (C2). We hence calculate the phonon frequencies and eigenvectors of the structures exemplified in Figs. 1(a) and 1(f), plus CH_2- and DPE-terminated carbynes of several lengths, using standard density-functional perturbation theory [11,25]. As a benchmark, our theoretical C-C stretching modes of polyynes C_nH_2 ($n = 8$–12) match the experimental frequencies [20] to within 40 cm^{-1}.

Besides several bending and long-wavelength stretching modes, whose low frequency falls in the same range as the vibrations of graphitic and diamondlike carbon material, short linear carbon chains display a few characteristic Raman-active stretching modes in the range $1800 \div 2300$ cm^{-1}. One mode, sometimes named the α mode in the literature [20], shows a displacement pattern localized near the chain center, and usually bears the strongest Raman intensity [20]. Since the displacements at the chain ends are less than 10% of those of the central atoms, the frequency of the α mode is almost unaffected by the mass of the termination (e.g., calculations for C_6H_4 and C_8H_4 with 1000-times increased hydrogen mass give frequency shifts of less than 1 cm^{-1}).

The stretching frequencies of sp chains turn out to be influenced by (i) the type of termination (sp^3 vs sp^2), (ii) the chain length, with even or odd alternating effects, and (iii) for sp^2 termination, the relative orientation of the termination themselves, with effects of torsional strain. The calculated frequencies of the high-energy Raman-active modes display a clear distinction between sp^2- and sp^3-terminated chains, as shown in Fig. 3. Only even-numbered chains are reported, since odd chains lack α modes, and have in general much smaller Raman cross sections [26].

Figure 3(c) displays the *in situ* Raman spectrum of an sp-sp^2 nanostructured-carbon film [5] in the carbyne region, measured using the 488 nm line of an Ar^+ laser and acquired with very high signal-to-noise ratio. The spectrum of the as-deposited material is compared to that obtained after exposure of the film to He in order to promote sp chain decay [27]. Clearly, a description in terms of two peaks only cannot account for the complex structure and decay observed. In particular, the C_p component at the highest frequency (peaked at 2260 cm^{-1}) can be attributed uniquely to short polyynic chains, as it is higher than any cumulenic α mode [see Fig. 3(a)], while the other components can be related both to polyynes and cumulenes of different length. As illustrated in Fig. 3(c), after He exposal, individual components have different evolutions

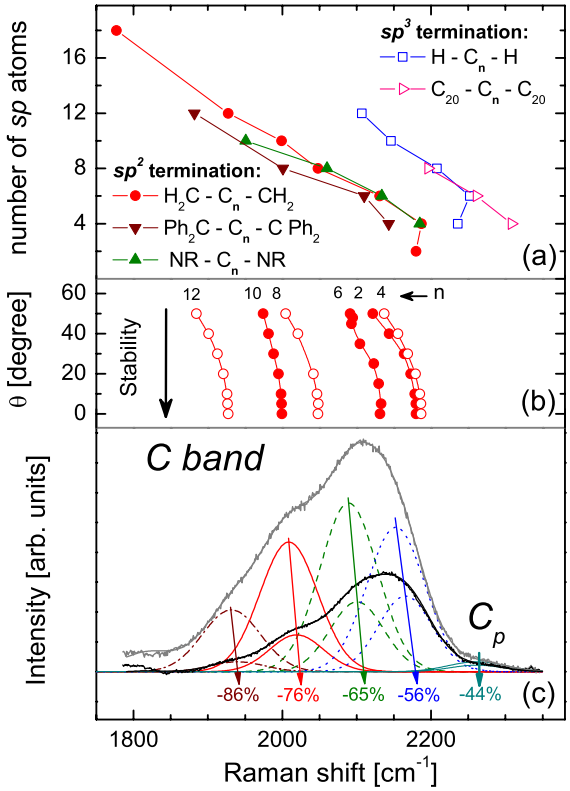

FIG. 3 (color online). (a) The computed frequency of the Raman α mode (horizontal scale) for carbon chains of different lengths n (vertical scale) and with different terminations. (b) The softening of this mode for CH_2-terminated chains as a function of the twist angle θ (vertical scale). (c) The experimental Raman spectra of pristine cluster-assembled sp-sp^2 film (top grey line) and of the same material after 2 days exposure to He, 100 Torr (black line). The underlying Gaussians report the empirical analysis of both spectra, resulting in 5 components at frequencies separated by approximately 80 cm^{-1}. The individual components display different decays, besides becoming narrower and undergoing a $\sim$10 cm^{-1} blueshift.

during the C band decay, and in particular, the peaks at lower energy, corresponding to longer chains, decay faster than the higher-energy ones (i.e., shorter chains). Furthermore, the C_p peak does not shift during the decay or change its width, while all lower peaks are blueshifted by $\sim 10\ \mathrm{cm}^{-1}$ and narrowed by $\sim 7\ \mathrm{cm}^{-1}$. Indeed calculations, summarized in Fig. 3(b), show that the high-frequency stretching modes of torsionally strained CH_2-terminated chains are affected quite strongly by the twist angle, with a redshift up to $\sim 100\ \mathrm{cm}^{-1}$. However, since chains with smaller torsional barrier (such as those bound to DPE and nanoribbons) show smaller redshifts, this effect evaluated for CH_2-terminated chains should be considered as an upper limit for realistic pure-carbon nanostructures.

The observed blueshift of the peaks accompanying the decay can then be explained if each peak is related to a particular family of cumulenes, having all the same length but different strain: the more strained chains, having softer Raman modes, decay faster than the others, resulting in a net blueshift and narrowing of the peak. A faster decay of torsionally strained vibrationally redshifted cumulene-type chains is indeed to be expected due to their higher total energy [Fig. 2(a)]. On the contrary, no torsional strain applies to polyynes, and this is why the C_p peak does not shift.

In summary, we performed *ab initio* total-energy and phonon calculations on a selected range of model structures sampling significantly the infinite variety of three-dimensional arrangements of linear carbon chains bridging graphitic fragments in different hybridization states. Theoretical results suggest that sp-carbon chains are stabilized, in particular, by bonding to the edges of graphitic nanofragments, and allow us to interpret the nontrivial features and decay of experimental Raman spectra of cluster-beam deposited pure-carbon films. Moreover, the data for sp^2-terminated chains point towards a rich phenomenology driven by even/odd alternation effects and by the effects of torsional strain. The latter modifies the electronic states near the Fermi level, suggesting the possibility to control the nanowire conductance [23], optical properties, and spin magnetization, purely by twisting its sp^2 termination, e.g., by coupling terminating graphene sheets with micromachined torsional actuators [28]. Linear carbon chains bridging graphene nanogaps, recently proposed as an explanation of the conductance switching in two-terminal graphene devices [3,4], could hence acquire an important role in future carbon-based electronics.

We acknowledge support by the Italian MIUR through PRIN-2006025747 and by the European Union through the ETSF-I3 project (Grant Agreement No. 211956/ETSF User Projects No. 62 and No. 124).

Note added in proof.—TEM images of chains similar to those depicted in Figs.1(a) and 1(c) have been recently reported in Ref. [29].

*Present address: Materials Science Department, University of Milan Bicocca, Via Cozzi 53, 20125 Milano, Italy
†giovanni.onida@mi.infn.it
‡pmilani@mi.infn.it

[1] Y.-M. Lin *et al.*, Nano Lett. **9**, 422 (2009).
[2] H. W. Ch. Postma, arXiv:0810.3035.
[3] B. Standley *et al.*, Nano Lett. **8**, 3345 (2008).
[4] Y. Li, A. Sinitskii, and J. M. Tour, Nature Mater. **7**, 966 (2008).
[5] L. Ravagnan *et al.*, Phys. Rev. Lett. **89**, 285506 (2002).
[6] L. Ravagnan *et al.*, Phys. Rev. Lett. **98**, 216103 (2007).
[7] N. D. Lang and Ph. Avouris, Phys. Rev. Lett. **81**, 3515 (1998); Phys. Rev. Lett. **84**, 358 (2000).
[8] Z. Qian *et al.*, Phys. Rev. B **78**, 113301 (2008).
[9] Ž. Crljen and G. Baranović, Phys. Rev. Lett. **98**, 116801 (2007).
[10] M. Weimer *et al.*, Chem. Phys. **309**, 77 (2005).
[11] P. Giannozzi *et al.*, http://www.quantum-espresso.org.
[12] We use the C.pz-rrkjus.UPF ultrasoft pseudopotential from Ref. [11] with a wave function or charge cutoff of 30/240 Ry, and relax all atomic positions until the largest residual force is $<2 \times 10^{-4}$ Ry$/a_0$ (8 pN). In the case of periodic graphene NRs, we adopt supercells with three hexagonal units along the periodic direction and at least 7 Å of vacuum separating periodic images in the two other directions, optimizing the lattice constant until the stress tensor drops below 2×10^{-5} Ry$/a_0^3$. We sample the Brillouin zone with at least 13 k points in each periodic direction and only $k = 0$ in nonperiodic directions. Numerical details are similar to those validated and used, e.g., in Ref. [13].
[13] T. Wassmann *et al.*, Phys. Rev. Lett. **101**, 096402 (2008).
[14] M. P. Bogana and L. Colombo, Appl. Phys. A **86**, 275 (2007).
[15] The BLA measures the degree of dimerization and, excluding the terminal bonds, can be defined as $\frac{1}{2}[\sum_{j=1}^{n_e}(d_{2j-1} + d_{n-(2j-1)})/n_e - \sum_{j=1}^{n_o}(d_{2j} + d_{n-2j})/n_o]$, with $d_i = |\vec{r}_i - \vec{r}_{i+1}|$, $n_e = (n+2)/4$, and $n_o = n/4$ (integer part).
[16] S. Okada, Phys. Rev. B **77**, 041408 (2008).
[17] Y. Liu *et al.*, Phys. Rev. B **68**, 125413 (2003).
[18] S. Eisler *et al.*, J. Am. Chem. Soc. **127**, 2666 (2005).
[19] T. Pino *et al.*, J. Chem. Phys. **114**, 2208 (2001).
[20] H. Tabata *et al.*, Carbon **44**, 3168 (2006).
[21] X. Gu, R. I. Kaiser, and A. M. Mebel, Chem. Phys. Chem. **9**, 350 (2008).
[22] S. Hino *et al.*, Chem. Phys. Lett. **372**, 59 (2003).
[23] K. H. Khoo *et al.*, Nano Lett. **8**, 2900 (2008).
[24] Odd-numbered chains show a reversed behavior, with high-spin states near the energetically unfavorable planar geometry $\theta \simeq 0°$.
[25] All phonon calculations start by fully relaxing all degrees of freedom except, in the case of torsionally strained $C_n(CH_2)_2$ systems, the angular coordinates of the H atoms around the molecular axis.
[26] For the simplest structures (CH_2-terminated chains) we also compute Raman intensities.
[27] C. S. Casari *et al.*, Phys. Rev. B **69**, 075422 (2004).
[28] J. A. Yeh *et al.*, J. Microelectromech. Syst. **8**, 456 (1999).
[29] C. Jin *et al.*, Phys. Rev. Lett. **102**, 205501 (2009).